European Journal of Radiology Open 7 (2020) 100297

Contents lists available at ScienceDirect

European Journal of Radiology Open

journal homepage: www.elsevier.com/locate/ejro

Influenza H1N1 virus-associated pneumonia often resembles rapidly progressive interstitial lung disease seen in collagen vascular diseases and COVID-19 pneumonia; CT-pathologic correlation in 24 patients

Makiko Murota [a,*], Takeshi Johkoh [b], Kyung Soo Lee [c], Tomas Franquet [d], Yasuhiro Kondoh [e], Yoshihiro Nishiyama [a], Tomonori Tanaka [f], Hiromitsu Sumikawa [g], Ryoko Egashira [h], Norihiko Yamaguchi [i], Kiminori Fujimoto [j], Junya Fukuoka [k], on behalf of the Group of Creation of Radiological Paper from Japan in diffuse lung disease

[a] Department of Radiology, Faculty of Medicine, Kagawa University, Kagawa, Japan
[b] Department of Radiology, Kansai Rosai Hospital, Hyogo, Japan
[c] Department of Radiology and Center for Imaging Science, Samsung Medical Center, Sungkyunkwan University School of Medicine, Seoul, Republic of Korea
[d] Department of Radiology, Hospital de Sant Pau, Universidad Autónoma de Barcelona, Barcelona, Spain
[e] Department of Respiratory and Allergic Medicine, Tosei General Hospital, Aichi, Japan
[f] Department of Pathology, Kindai University Faculty of Medicine, Osaka, Japan
[g] Department of Radiology, Sakai City Medical Center, Osaka, Japan
[h] Department of Radiology, Faculty of Medicine, Saga University, Saga, Japan
[i] Department of Respiratory Medicine, Kinki Central Hospital of Mutual Aid Association of Public School Teachers, Hyogo, Japan
[j] Department of Radiology, Kurume University School of Medicine, Fukuoka, Japan
[k] Department of Laboratory of Pathology, Nagasaki University Hospital, Nagasaki, Japan

ARTICLE INFO

Keywords:
Influenza A (H1N1) virus
Computed tomography
Pneumonia
Myositis and muscle disease
Rheumatoid arthritis
COVID-19

ABSTRACT

Purpose: To describe computed tomography (CT) findings of influenza H1N1 virus-associated pneumonia (IH1N1VAP), and to correlate CT findings to pathological ones.

Methods: The study included 24 patients with IH1N1VAP. Two observers independently evaluated the presence, distribution, and extent of CT findings. CT features were divided into either classical form (C-form) or non-classical form (NC-form). C-form included: A.) broncho-bronchiolitis and bronchopneumonia type, whereas NC-forms included: B.) diffuse peribronchovascular type, simulating subacute rheumatoid arthritis-associated (RA) interstitial lung disease (ILD) and C.) lower peripheral and/or peribronchovascular type, resembling dermatomyositis-associated ILD and COVID-19 pneumonia. In 10 cases with IH1N1VAP where lung biopsy was performed, CT and pathology findings were correlated.

Results: The most common CT findings were ground-glass opacities (24/24, 100 %) and airspace consolidation (23/24, 96 %). C-form was found in 11 (46 %) patients while NC-form in 13 (54 %). Types A, B, and C were seen in 11(46 %), 4 (17 %), and 9 (38 %) patients, respectively. The lung biopsy revealed organizing pneumonia in all patients and 6 patients (60 %) showed incorporated type organizing pneumonia that was common histological findings of rapidly progressive ILD.

Conclusion: In almost half of patients of IH1N1VAP, CT images show NC-form pneumonia pattern resembling either acute or subacute RA or dermatomyositis-associated ILD and COVID-19 pneumonia.

1. Introduction

Influenza A (H1N1) virus infection is reported an outbreak in Mexico in April 2009 [1]. Since then it has spread rapidly worldwide. This pandemic influenza caused increased morbidity and mortality in a young population who were not generally at risk for severe illness with the usual seasonal influenza [1]. The most common causes of death due to H1N1 infection are pneumonia and acute respiratory distress

* Corresponding author at: Department of Radiology, Faculty of Medicine, Kagawa University, 1750-1 Ikenobe, Miki-cho, Kita-gun, Kagawa, 761-0793, Japan.
E-mail address: mwada@med.kagawa-u.ac.jp (M. Murota).

https://doi.org/10.1016/j.ejro.2020.100297
Received 12 October 2020; Received in revised form 18 November 2020; Accepted 23 November 2020
Available online 28 November 2020

syndrome [2]. The main pathological finding in patients with H1N1 infection was reported to be exudative diffuse alveolar damage (DAD) with variable degrees of pulmonary hemorrhage and necrotizing bronchiolitis [3,4]. There are also few case reports describing pathological findings of organizing pneumonia (OP) associated with influenza A (H1N1) virus infection [2,5]. Moreover, Cornejo et al. [5] suggested that the clinical symptoms of severe respiratory failure observed in these patients do not seem to resemble those of OP due to other causes.

In patients of interstitial lung disease with dermatomyositis (DM), polymyositis and antisynthetase syndrome (ASS), it has been reported OP with supervening fibrosis described in the American Thoracic Society and European Respiratory Society (ATS/ERS) statement [6,7]. Its characteristic computed tomography (CT) findings are regions of airspace consolidation bilaterally that show prominent loss of volume, and distribution predominantly in the basal segments. In patients with OP with fibrosis, the condition was reported to develop rapidly progressive interstitial lung disease (RPILD), and be resistant to therapy [6,8].

Recently, novel coronavirus (COVID-19) causes worldwide pandemic and critics in the world. COVID-19 pneumonia often shows bilateral subpleural ground-glass attenuation and /or airspace consolidation and severe one depicts lower lobe predominant airspace consolidation with loss of volume and traction broncho-bronchiolectasis [9,10]

Several studies have been reported on radiological features of influenza A (H1N1) pneumonia. The most common CT findings are ground-glass opacities (GGO) and consolidation, with predominant peribronchovascular and subpleural distribution, resembling OP [2,11,12]. However, few studies have evaluated radiologic and pathologic findings of lung specimens. Marchiori et al. [13] reported a correlation between CT and pathologic findings in six adult patients who died following Influenza A (H1N1) pneumonia. They concluded that fatal cases of Influenza A (H1N1) pneumonia can present areas of consolidation on CT and can be pathologically correlated with DAD [13]. However, the detailed CT findings and their correlation with pathologic findings in patients with influenza A (H1N1) pneumonia is still unknown. The aim of this study was to describe the HRCT findings in patients with Influenza A (H1N1) pneumonia and to correlate them in detail with the pathological features.

2. Materials and methods

2.1. Description of CT findings

2.1.1. Patients

The institutional review board of the lead institution, where this study was carried out, approved this retrospective study and waived the need for obtaining the consent of individual patients. We reviewed the medical records in our databases of all the patients seen in four institutions. The study included 24 patients (14 males and 10 females; 18–86 years of age, 58 years on average) who were identified with influenza A (H1N1) pneumonia between March 2009 and September 2017. The patients were diagnosed based on positive results of real-time polymerase chain reaction (RT-PCR) or PCR on nasal swab or respiratory specimen for influenza A (H1N1). And combined infections were excluded due to a negative sputum and/or blood culture for other pathogens. None of all patients had clinically collagen vascular diseases.

2.1.2. CT scanning

Thin-section CT was performed using a variety of CT scanners. Data acquisition was obtained on inspiration, with the patient in the supine position. The protocols consisted of 1- or 2.5-mm collimation sections reconstructed at 1- or 2-mm intervals. The images were viewed at window settings optimized for lung (window level −550 to -600 Hounsfield units [HU], window width 1500–1600 HU) and the mediastinum (window level 300–350 HU, window width30 to 40 HU).

2.1.3. Image analysis

The images were retrospectively reviewed independently by two chest radiologists with 18- and 30- years of experience. The radiologists were aware that the patients had influenza A (H1N1) pneumonia, but were blinded to any other clinical information. Radiologists evaluated the CT findings, including the extent of spared areas, as follows: GGO, airspace consolidation, intralobular reticular opacities, emphysema, and bronchial dilatation. In addition, the presence of bronchial wall thickening, loss of volume in the lower lung zones, subpleural sparing, centrilobular nodules, tree-in-bud appearance, lymphadenopathy, and pleural effusion was evaluated. The definitions of these CT findings were based on the literature [7,14,15], as follows: intralobular reticular opacities were defined as irregular and randomized linear shadows separated by a few millimeters; subpleural sparing was defined as an area of relative sparing adjacent to the pleura in the presence of fibrotic changes in the lung field; and upper lobe subpleural irregular lines were defined as irregular lines adjacent to the pleura in the upper lobes. The extent of CT findings was evaluated separately for 6 pulmonary zones (upper, middle, and lower on each side). The anatomical distribution was classified as unilateral or bilateral, as predominantly peripheral if the lesion was in the outer one-third of the lung, as peribronchovascular if there was a predominance of abnormalities along the bronchovascular bundles, or random. The borders between the upper and middle, and between middle and lower lung zones were divided by the level of the tracheal carina and the inferior pulmonary vein, respectively. The radiologists estimated the percentage of lung with abnormalities in each of the zones, which included spared areas, ground-glass attenuation with and without traction bronchiectasis, airspace consolidation, intralobular reticular opacities, and emphysema. The percentage of whole lung involved with abnormalities was calculated by determining the mean of the percentages of involved lung in each lung zone.

Through reviewing all CT images, CT features were divided into either classical or non-classical forms. The classical form included: A.) broncho-bronchiolitis and bronchopneumonia type (Fig. 1), showing segmental centrilobular nodules and/or areas of airspace consolidation, whereas the non-classical forms included: B.) diffuse peribronchovascular type (Fig. 2), depicting areas with ground-glass opacities (GGO) or airspace consolidation diffusely distributed along bronchovascular bundles simulating subacute rheumatoid arthritis-associated (RA) interstitial lung disease [16] and C.) lower peripheral and/or peribronchovascular type (Figs. 3 and 4), showing areas of airspace consolidation along pleura and/or peribronchovascular area in bilateral lower lung zones resembling DM-associated interstitial lung disease and COVID-19 pneumonia [9,10,17].

2.1.4. Statistical analysis

Statistical analysis was performed using SPSS Statistics software (Version 24, 2016; IBM Corp. Japan). Interobserver agreement regarding the presence/absence of CT findings and overall impression of the findings was analyzed by calculating the kappa statistic on the assessments made prior to agreement by consensus, by the chest radiologist who reviewed the images. Interobserver agreement was classified as follows: poor ($\kappa = 0-0.20$), fair ($\kappa = 0.21-0.40$), moderate ($\kappa = 0.41-0.60$), substantial ($\kappa = 0.61-0.80$), and excellent ($\kappa = 0.81-1.00$).

2.2. Radiologic-pathologic correlation

We retrospectively reviewed medical records of patients seen at two institutions between J March 2009 and September 2017, and identified ten (five males and five females; 33–71 years of age, 52 years on average) patients who had influenza A (H1N1) virus pneumonia and had undergone lung biopsy. These were two cases of surgical lung biopsy and eight cases of transbronchial cryobiopsy. Pathological patterns were described by ATS/ERS classification [6], such as DAD, OP, etc. As far as OP, we further categorized two subtypes, intraluminal and incorporated

Fig. 1. 72-Year-old man with influenza A (H1N1) pneumonia.
CT shows airspace consolidation, centrilobular nodules, and tree-in-bud appearance (categorized as type A).

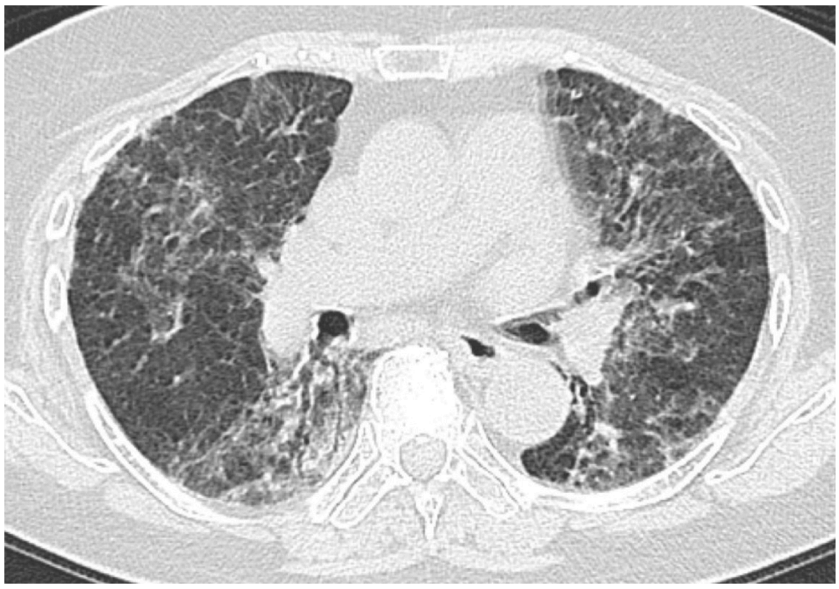

Fig. 2. 86-Year-old woman with influenza A (H1N1) pneumonia.
CT shows GGO diffusely distribute along peribronchovascular opacities, simulating subacute rheumatoid arthritis-associated interstitial lung disease (categorized as type B).

type, according to the previous reports [18,19]. Namely, intraluminal OP is characteristic of intraluminal polypoid immature fibrotic lesion (Masson type polyp) while incorporated one demonstrated intraluminal fibrotic lesions incorporated into the alveolar wall. The radiologic-pathologic correlation was performed together by one radiologist with 30-years of experience and one pathologist with nine-years of experience. The radiologist reviewed CT images and categorized into the three types mentioned above under Image Analysis. The 10 cases were used for precise radiologic pathologic correlation, including to distinguish pathologic type of OP.

3. Results

3.1. Description of CT findings

CT findings are shown in Table 1. The main CT findings were GGO (100 %) and airspace consolidation (96 %), which were bilateral (71 %), lower (63 %), along the peribronchovascular (83 %), or peripheral (29 %). They were followed by lymphadenopathy (50 %), centrilobular nodules (46 %), lower volume loss (42 %), subpleural sparing (33 %), tree-in-bud appearance (29 %), bronchial wall thickening (29 %), and pleural effusion (29 %). Non-classical form was seen in 13 (54 %) of 24 patients, slightly higher than classical forms that were observed in 11 patients (46 %). Types A (Fig. 1), B (Fig. 2), and C (Fig. 3,4) were seen in 11 (46 %), 4 (17 %), and 9 (38 %) patients, respectively. The interobserver agreement for identification of CT forms was substantial ($\kappa = 0.75$).

3.2. Radiologic-pathologic correlation

In 10 patients who underwent lung biopsy, CT images in four showed classical form (type A) and in six cases non-classical forms including one

Fig. 3. 76-Year-old woman with influenza A (H1N1) pneumonia.
CT shows areas of GGO and airspace consolidation along pleura in bilateral lower lung zones, resembling dermatomyositis-associated interstitial lung disease (categorized into type C).

cases of type B and five cases of type C. All these cases pathologically showed OP. Six patients demonstrated incorporated type of OP where granulation tissue incorporated into the alveolar wall with various degree of inflammatory cells. Three patients (30 %) demonstrated intraluminal type OP. One patient (10 %) has admixture of intraluminal and incorporated OP. CT pattern of type A included three incorporated and one intraluminal OP, type B included one combined incorporated and intraluminal OP, type C included three incorporated OP and two intraluminal OP. In this cohort, no patients showed DAD, hemorrhage and necrotizing bronchiolitis.

4. Discussion

In this study, we evaluated the CT images of 24 patients with influenza A (H1N1) pneumonia. The observed CT features were divided into either classical form or non-classical forms. Further, the classical form included: A.) broncho-bronchiolitis and bronchopneumonia type, showing segmental centrilobular nodules and/or areas of airspace consolidation, whereas the non-classical forms included: B.) diffuse peribronchovascular type, depicting areas with GGO or airspace consolidation diffusely distributed along bronchovascular bundles simulating subacute RA interstitial lung disease and C.) lower peripheral and/or peribronchovascular type, showing areas of airspace consolidation along pleura and/or peribronchovascular area in bilateral lower lung zones resembling DM-associated interstitial lung disease. The lung biopsy revealed OP in all 10 patients and 6 patients (60 %) showed incorporated type OP that was common histological findings seen in DM and ASS.

There have been many reports on CT findings of influenza A (H1N1) virus pneumonia [12,20,21]. Previous reports [12,20,21] showed that the most frequent CT findings were the presence of extensive GGO and airspace consolidation, and also the existence of centrilobular nodules, and tree-in-bud appearance as broncho-bronchiolitis and bronchopneumonia. In contrast, Kang et al. [22] reported patterns of CT findings in influenza A (H1N1) pneumonia, and classified them into 3 patterns: bronchopneumonia, cryptogenic OP, and acute interstitial pneumonia. However, in the present study, we have described for the first time not only the CT patterns but also about their correlation with pathology of influenza A (H1N1) pneumonia.

In the present study, non-classical forms were seen in almost half of patients and were slightly higher than in classical form that is type A. Li et al. [21] and Ajlan et al. [11] reported the distribution of peribronchovascular and peripheral distribution of influenza A (H1N1) pneumonia and discussed that appearance was similar to that seen in cases of OP on CT. We classified non-classical forms into type B and type C. Diffuse peribronchovascular opacities on CT as type B, also called “twisted appearance” were previously described in subacute RA interstitial lung disease [16]. The proximal airway is known to be affected in RA interstitial lung disease and drug pneumonitis [16,23]. On the other hand, lower peripheral and/or peribronchovascular patterns showing areas of airspace consolidation along pleura and/or peribronchovascular in bilateral lower lung zones as type C was reported as CT findings in DM-associated interstitial lung disease [7,17,24,25]. However, if CT images of patients with influenza A (H1N1) pneumonia show non-classical forms, it is difficult to differentiate findings of influenza A (H1N1) pneumonia from other viral pneumonia such as severe acute respiratory syndrome (SARS), Middle East respiratory syndrome (MERS), and coronavirus disease (COVID-19) pneumonia [26–28]. Yin et al. investigated to compare the CT findings of influenza A (H1N1) pneumonia and COVID-19 pneumonia and reported that peripheral or peribronchovascular distribution, GGO, and consolidation were not significantly different between them [28]. The CT finding in patients with MERS and SARS was reported that the distribution of the abnormalities, such as GGO and consolidation, to the subpleural and peribronchovascular regions is suggestive of organizing pneumonia pattern [26,27].

In our study, although OP was seen in all patients, DAD was not observed. In past reports, the main pathological findings in patients with influenza A (H1N1) pneumonia include DAD with variable degrees of pulmonary hemorrhage and necrotizing bronchiolitis [3]. Our cohort include cryobiopsy which is smaller than surgical lung biopsy, so DAD may be missed. We think current cohort consisted with relatively mild disease of influenza A (H1N1) pneumonia, the histological discrepancy may be due to the difference in inclusion criteria. Recently, however, there have been a few case reports described pathologic findings of OP associated with influenza A (H1N1) pneumonia [2,5,29,30]. Moreover,

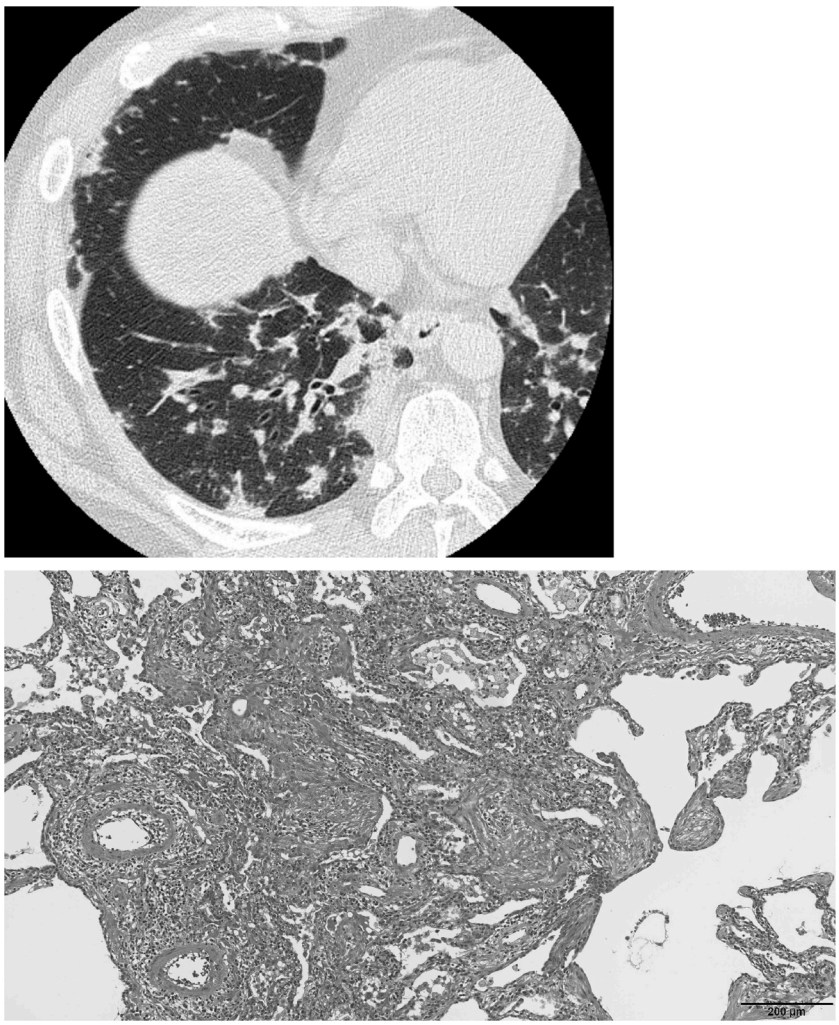

Fig. 4. 45-Year-old man with influenza A (H1N1) pneumonia. Radiologic-pathologic correlation (type C).
(A) CT shows areas of GGO and airspace consolidation along pleura and peribronchovascular zone bilaterally in lower lung resembling dermatomyositis-associated interstitial lung disease (categorized into type C) (B) Photomicrograph shows organizing pneumonia of incorporated pattern (hematoxylin-eosin).

Cornejo et al. [5] alerted about the possibility of OP associated with influenza A (H1N1) pneumonia in patients with severe respiratory failure. In these patients, the authors also discussed that the clinical symptoms of severe respiratory failure observed do not seem to resemble those of OP due to other causes.

Histologically, OP is characterized by the presence of granulation tissue (inflammatory cells, fibroblasts and loose connective tissue) in the alveoli and alveolar ducts [31]. Histological OP is considered a nonspecific tissue reaction to various causes of lung injury, including drugs, radiation, connective tissue diseases, cancers, lung and bone marrow transplantation, and bacterial or virus infection [5,31]. A case of COVID-19 pneumonia was also reported which the presence of organizing pneumonia confirmed histologically [32]. A few reports described pathologically a “bronchiolitis obliterans organizing pneumonia (BOOP)-like pattern” in patients with SARS [33]. Some investigators have indicated that secondary OP associated with collagen vascular diseases has a poorer prognosis than cryptogenic OP [31,34,35]. Histological OP has two subtypes, intraluminal type OP and incorporated type OP [18,19]. In recent reports, it was described that incorporated type OP was observed in patients of RPILD with DM and ASS [36,37]. Current study revealed for the first time that patients with influenza A (H1N1) pneumonia frequently demonstrate incorporated type OP as well. From the histological viewpoint, RPILD of DM/ASS and influenza A (H1N1) pneumonia have common features. In order to confirm this result, it is necessary to verify with more surgical lung biopsy cases of influenza A (H1N1) pneumonia. This may be related to a poor prognosis in influenza A (H1N1) pneumonia as in patients with DM-associated interstitial lung disease and ASS interstitial lung disease.

We surprisingly found that incorporated OP was pathologically seen not only in cases with non-classical forms (type B and C) but also with classical form (type A). The reason for this finding is unclear, however, it is possible that the cases with type A may represent a milder form than the type B and C.

The appearance of anti-melanoma differentiation associated gene 5 (MDA5) antibody was reported to be associated with rapidly progressive interstitial lung disease caused by clinically amyopathic DM [38]. MDA5 is one of the retinoic acid-inducible gene I (RIG-I) like receptors (RLRs), which are involved in the recognition of viral RNAs and play an important role in innate immune response. RIG-I is also one of the RLRs reported to be essential for the production of interferons in response to RNA viruses including influenza virus, whereas MDA5 is critical for picornavirus detection [39]. However, it was recently reported the RIG-I is not only primary pattern recognition receptor for influenza A virus but implicated MDA5 is also as a significant contributor to the cellular defense against influenza A virus [40]. Thus, CT findings of influenza A (H1N1) pneumonia in the present study may be similar to those of dermatomyositis-associated interstitial lung disease.

Our study had several limitations. First, it was a retrospective study,

Table 1
CT findings of influenza H1N1 virus-associated pneumonia.

CT findings	Number of patients		κ
Ground-glass opacities	24/24 (100)		N.A.
Airspace consolidation	23/24 (96)		0.36
Intralobular reticular opacities	1/24 (4)		0.16
Emphysema	1/24 (4)		0.36
Bronchial dilatation	2/24 (8)		−0.14
Bronchial wall thickening	7/24 (29)		0.48
Lower volume loss	10/24 (42)		0.41
Subpleural sparing	8/24 (33)		0.00
Centrilobular nodules	11/24 (46)		0.66
Tree-in-bud appearance	7/24 (29)		0.65
Lymphadenopathy	12/24 (50)		0.25
Pleural effusion	7/24 (29)		0.73
Predominant overall anatomic distribution			
Peripheral	7/24 (29)		0.63
Peribronchovascular	20/24 (83)		0.21
Bilateral	17/24 (71)		0.36
Unilateral	7/24 (29)		0.36
Lower	15/24 (63)		0.50
Upper and middle	4/24 (17)		0.25
Diffuse or random	5/24 (21)		0.19
CT pattern			
Classical (type A)	11/24 (46)		0.75
Non-classical (type B)	4/24 (17)	13/24 (54)	0.75
Non-classical (type C)	9/24 (38)		

which introduced an inherent selection bias. We evaluated patients with influenza A (H1N1) pneumonia who underwent CT scan. This group may include more severe patients and/or more non-classical type than the group of not undergoing CT scan. Similarly, in patients with influenza A (H1N1) pneumonia in whom lung biopsy was performed, it was possible to be showed clinically severe or atypical manifestation. Second, it included a relatively small number of patients. Finally, regarding the radiologic-pathologic correlation, the cryobiopsy may not be enough for histological evaluation because the size is smaller than surgical lung biopsy.

5. Conclusion

In conclusion, in almost half of patients with H1N1 pneumonia, CT images showed non-classical form pneumonia patterns similar to either acute or subacute RA interstitial lung disease, DM-associated interstitial lung disease, or COVID-19 pneumonia. Moreover, in H1N1 influenza pneumonia patients, not only CT findings but also histological features demonstrate common characteristic to RPILD seen in DM and ASS.

Informed consent

The Ethics Committee of Kagawa University Hospital, that is the institutional review board of the lead institution, approved this retrospective study and waived the need for obtaining the consent of individual patients.

Funding

This research did not receive any specific grant from funding agencies in the public, commercial, or not-for-profit sectors.

CRediT authorship contribution statement

Makiko Murota: Supervision, Methodology, Writing - original draft. **Takeshi Johkoh:** Conceptualization, Methodology, Resources, Writing - review & editing. **Kyung Soo Lee:** Resources, Investigation. **Tomas Franquet:** Resources, Investigation. **Yasuhiro Kondoh:** Resources, Investigation. **Yoshihiro Nishiyama:** Writing - review & editing. **Tomonori Tanaka:** Investigation. **Hiromitsu Sumikawa:** Investigation. **Ryoko Egashira:** Writing - review & editing. **Norihiko Yamaguchi:** Resources, Investigation. **Kiminori Fujimoto:** Writing - review & editing. **Junya Fukuoka:** Writing - review & editing.

Declaration of Competing Interest

The authors report no declarations of interest.

Acknowledgements

This study was performed on the behalf of the Study Group of Creation of Radiological Paper from Japan in Diffuse Lung Disease. The members are as follows: Hiroaki Arakawa, Ryoko Egashira, Kiminori Fujimoto, Junya Fukuoka, Hiroto Hatabu, Kazuya Ichikado, Tae Iwasawa, Takeshi Johkoh, Yasuhiro Kondoh, Makiko Murota, Takashi Ogura, Fumikazu Sakai, Hiroaki Sugiura, Hiromitsu Sumikawa, Hiroyuki Taniguchi, Junya Tominaga, Noriyuki Tomiyama.

References

[1] R. Perez-Padilla, D. de la Rosa-Zamboni, S. Ponce de Leon, M. Hernandez, F. Quiñones-Falconi, E. Bautista, A. Ramirez-Venegas, J. Rojas-Serrano, C. E. Ormsby, A. Corrales, A. Higuera, E. Mondragon, J.A. Cordova-Villalobos, INER Working Group on Influenza, Pneumonia and respiratory failure from swine-origin influenza a (H1N1) in Mexico, N. Engl. J. Med. 361 (2009) 680–689, https://doi.org/10.1056/NEJMoa0904252.

[2] A. Torrego, V. Pajares, A. Mola, E. Lerma, T. Franquet, Influenza A (H1N1) organising pneumonia, Case Rep. 2010 (2010), https://doi.org/10.1136/bcr.12.2009.2531 bcr1220092531–bcr1220092531.

[3] T. Mauad, L.A. Hajjar, G.D. Callegari, L.F.F. da Silva, D. Schout, F.R.B.G. Galas, V. A.F. Alves, D.M.A.C. Malheiros, J.O.C. Auler, A.F. Ferreira, M.R.L. Borsato, S. M. Bezerra, P.S. Gutierrez, E.T.E.G. Caldini, C.A. Pasqualucci, M. Dolhnikoff, P.H. N. Saldiva, Lung pathology in fatal novel human influenza a (H1N1) infection, Am. J. Respir. Crit. Care Med. 181 (2010) 72–79, https://doi.org/10.1164/rccm.200909-1420OC.

[4] N. Nin, C. Sánchez-Rodríguez, L.S. Ver, P. Cardinal, A. Ferruelo, L. Soto, A. Deicas, N. Campos, O. Rocha, D.H. Ceraso, M. El-Assar, J. Ortín, P. Fernández-Segoviano, A. Esteban, J.A. Lorente, Lung histopathological findings in fatal pandemic influenza A (H1N1), Med. Intensiva 36 (2012) 24–31, https://doi.org/10.1016/j.medin.2011.10.005.

[5] R. Cornejo, O. Llanos, C. Fernandez, J. Carlos Diaz, G. Cardemil, J. Salguero, C. Luengo, E. Tobar, C. Romero, L.R. Galvez, Organizing pneumonia in patients with severe respiratory failure due to novel A (H1N1) influenza, BMJ Case Rep. 2010 (2010), https://doi.org/10.1136/bcr.02.2010.2708.

[6] W.D. Travis, U. Costabel, D.M. Hansell, T.E. King, D.A. Lynch, A.G. Nicholson, C. J. Ryerson, J.H. Ryu, M. Selman, A.U. Wells, J. Behr, D. Bouros, K.K. Brown, T. V. Colby, H.R. Collard, C.R. Cordeiro, V. Cottin, B. Crestani, M. Drent, R.F. Dudden, J. Egan, K. Flaherty, C. Hogaboam, Y. Inoue, T. Johkoh, D.S. Kim, M. Kitaichi, J. Loyd, F.J. Martinez, J. Myers, S. Protzko, G. Raghu, L. Richeldi, N. Sverzellati, J. Swigris, D. Valeyre, ATS/ERS Committee on Idiopathic Interstitial Pneumonias, An official American Thoracic Society/European respiratory society statement: update of the international multidisciplinary classification of the idiopathic interstitial pneumonias, Am. J. Respir. Crit. Care Med. 188 (2013) 733–748, https://doi.org/10.1164/rccm.201308-1483ST.

[7] Y. Waseda, T. Johkoh, R. Egashira, H. Sumikawa, K. Saeki, S. Watanabe, R. Matsunuma, H. Takato, Y. Ichikawa, Y. Hamaguchi, A. Shiraki, Y. Muro, M. Yasui, H. Prosch, C. Herold, K. Kasahara, Antisynthetase syndrome: pulmonary computed tomography findings of adult patients with antibodies to aminoacyl-tRNA synthetases, Eur. J. Radiol. 85 (2016) 1421–1426, https://doi.org/10.1016/j.ejrad.2016.05.012.

[8] Y. Kondoh, H. Taniguchi, K. Kataoka, K. Kato, R. Suzuki, T. Ogura, T. Johkoh, T. Yokoi, A.U. Wells, M. Kitaichi, Tokai Diffuse Lung Disease Study Group, Prognostic factors in rapidly progressive interstitial pneumonia, Respirology 15 (2010) 257–264, https://doi.org/10.1111/j.1440-1843.2009.01687.x.

[9] Y. Wang, C. Dong, Y. Hu, C. Li, Q. Ren, X. Zhang, H. Shi, M. Zhou, Temporal changes of CT findings in 90 patients with COVID-19 pneumonia: a longitudinal study, Radiology 296 (2020) E55–E64, https://doi.org/10.1148/radiol.2020200843.

[10] K. Li, J. Wu, F. Wu, D. Guo, L. Chen, Z. Fang, C. Li, The clinical and chest CT features associated with severe and critical COVID-19 pneumonia, Invest. Radiol. 55 (2020) 327–331, https://doi.org/10.1097/RLI.0000000000000672.

[11] A.M. Ajlan, B. Quiney, S. Nicolaou, N.L. Müller, Swine-origin influenza a (H1N1) viral infection: radiographic and CT findings, Am. J. Roentgenol. 193 (2009) 1494–1499, https://doi.org/10.2214/AJR.09.3625.
[12] E. Marchiori, G. Zanetti, G. D'Ippolito, C.G.Y. Verrastro, G. de S.P. Meirelles, J. Capobianco, R.S. Rodrigues, Swine-origin influenza A (H1N1) viral infection: thoracic findings on CT, AJR Am. J. Roentgenol. 196 (2011) W723–728, https://doi.org/10.2214/AJR.10.5109.
[13] E. Marchiori, G. Zanetti, C.A.P. Fontes, M.L.O. Santos, P.M. Valiante, C.M. Mano, G.H.C. Teixeira, B. Hochhegger, Influenza A (H1N1) virus-associated pneumonia: high-resolution computed tomography-pathologic correlation, Eur. J. Radiol. 80 (2011) 500–504, https://doi.org/10.1016/j.ejrad.2010.10.003.
[14] H. Sumikawa, T. Johkoh, T.V. Colby, K. Ichikado, M. Suga, H. Taniguchi, Y. Kondoh, T. Ogura, H. Arakawa, K. Fujimoto, A. Inoue, N. Mihara, O. Honda, N. Tomiyama, H. Nakamura, N.L. Müller, Computed tomography findings in pathological usual interstitial pneumonia: relationship to survival, Am. J. Respir. Crit. Care Med. 177 (2008) 433–439, https://doi.org/10.1164/rccm.200611-1696OC.
[15] M. Akira, Y. Inoue, M. Kitaichi, S. Yamamoto, T. Arai, K. Toyokawa, Usual interstitial pneumonia and nonspecific interstitial pneumonia with and without concurrent emphysema: thin-section CT findings, Radiology 251 (2009) 271–279, https://doi.org/10.1148/radiol.2511080917.
[16] E. Watanabe, T. Kawamura, Y. Mochizuki, Y. Nakahara, S. Sasaki, A. Okamoto, T. Higashino, Consolidation with a twisted appearance along the airways: a report of five cases of interstitial pneumonia, Respir. Investig. 52 (2014) 213–218, https://doi.org/10.1016/j.resinv.2013.12.006.
[17] K. Tanizawa, T. Handa, R. Nakashima, T. Kubo, Y. Hosono, K. Watanabe, K. Aihara, T. Oga, K. Chin, S. Nagai, T. Mimori, M. Mishima, HRCT features of interstitial lung disease in dermatomyositis with anti-CADM-140 antibody, Respir. Med. 105 (2011) 1380–1387, https://doi.org/10.1016/j.rmed.2011.05.006.
[18] B. Beardsley, D. Rassl, Fibrosing organising pneumonia, J. Clin. Pathol. 66 (2013) 875–881, https://doi.org/10.1136/jclinpath-2012-201342.
[19] T. Yoshinouchi, Y. Ohtsuki, K. Kubo, Y. Shikata, Clinicopathological study on two types of cryptogenic organizing pneumonitis, Respir. Med. 89 (1995) 271–278 (Accessed January 5, 2019), http://www.ncbi.nlm.nih.gov/pubmed/7597266.
[20] N. Tanaka, T. Emoto, H. Suda, Y. Kunihiro, N. Matsunaga, S. Hasegawa, T. Ichiyama, High-resolution computed tomography findings of influenza virus pneumonia: a comparative study between seasonal and novel (H1N1) influenza virus pneumonia, Jpn. J. Radiol. 30 (2012) 154–161, https://doi.org/10.1007/s11604-011-0027-6.
[21] P. Li, D.-J. Su, J.-F. Zhang, X.-D. Xia, H. Sui, D.-H. Zhao, Pneumonia in novel swine-origin influenza A (H1N1) virus infection: high-resolution CT findings, Eur. J. Radiol. 80 (2011) e146–e152, https://doi.org/10.1016/j.ejrad.2010.05.029.
[22] H. Kang, K.S. Lee, Y.J. Jeong, H.Y. Lee, K. Il Kim, K.J. Nam, Computed tomography findings of influenza a (H1N1) pneumonia in adults, J. Comput. Assist. Tomogr. 36 (2012) 285–290, https://doi.org/10.1097/RCT.0b013e31825588e6.
[23] C.I.S. Silva, N.L. Müller, Drug-induced lung diseases: most common reaction patterns and corresponding high-resolution CT manifestations, Semin. Ultrasound CT MR 27 (2006) 111–116 (Accessed November 4, 2018), http://www.ncbi.nlm.nih.gov/pubmed/16623365.
[24] M.-P. Debray, R. Borie, M.-P. Revel, J.-M. Naccache, A. Khalil, C. Toper, D. Israel-Biet, C. Estellat, P.-Y. Brillet, Interstitial lung disease in anti-synthetase syndrome: initial and follow-up CT findings, Eur. J. Radiol. 84 (2015) 516–523, https://doi.org/10.1016/j.ejrad.2014.11.026.
[25] S. Karadimitrakis, S.C. Plastiras, A. Zormpala, K. Chatzikonstantinou, K.A. Boki, G. E. Tzelepis, H.M. Moutsopoulos, Chest CT findings in patients with inflammatory myopathy and Jo1 antibodies, Eur. J. Radiol. 66 (2008) 27–30, https://doi.org/10.1016/j.ejrad.2007.05.017.
[26] G.C. Ooi, P.L. Khong, N.L. Müller, W.C. Yiu, L.J. Zhou, J.C.M. Ho, B. Lam, S. Nicolaou, K.W.T. Tsang, Severe acute respiratory syndrome: temporal lung changes at thin-section CT in 30 patients, Radiology 230 (2004) 836–844, https://doi.org/10.1148/radiol.2303030853.
[27] A.M. Ajlan, R.A. Ahyad, L.G. Jamjoom, A. Alharthy, T.A. Madani, Middle East respiratory syndrome coronavirus (MERS-CoV) infection: chest CT findings, AJR Am. J. Roentgenol. 203 (2014) 782–787, https://doi.org/10.2214/AJR.14.13021.
[28] Z. Yin, Z. Kang, D. Yang, S. Ding, H. Luo, E. Xiao, A comparison of clinical and chest CT findings in patients with influenza a (H1N1) virus infection and coronavirus disease (COVID-19), AJR Am. J. Roentgenol. (2020) 1–7, https://doi.org/10.2214/AJR.20.23214.
[29] A. Gómez-Gómez, R. Martínez-Martínez, M.B. Gotway, Organizing pneumonia associated with swine-origin influenza a H1N1 2009 viral infection, Am. J. Roentgenol. 196 (2011) W103–W104, https://doi.org/10.2214/AJR.10.4689.
[30] E. Marchiori, G. Zanetti, F.A. Ferreira Francisco, B. Hochhegger, Organizing pneumonia as another pathological finding in pandemic influenza A (H1N1), Med. Intensiva 37 (2013) 59, https://doi.org/10.1016/j.medin.2012.08.002.
[31] G.R. Epler, T.V. Colby, T.C. McLoud, C.B. Carrington, E.A. Gaensler, Bronchiolitis obliterans organizing pneumonia, N. Engl. J. Med. 312 (1985) 152–158, https://doi.org/10.1056/NEJM198501173120304.
[32] B.P. Pogatchnik, K.E. Swenson, H. Sharifi, H. Bedi, G.J. Berry, H.H. Guo, Radiology-pathology correlation in recovered COVID-19, demonstrating organizing pneumonia, Am. J. Respir. Crit. Care Med. 202 (2020), https://doi.org/10.1164/rccm.202004-1278IM.
[33] W.-F. Ng, K.-F. To, W.W.L. Lam, T.-K. Ng, K.-C. Lee, The comparative pathology of severe acute respiratory syndrome and avian influenza A subtype H5N1–a review, Hum. Pathol. 37 (2006) 381–390, https://doi.org/10.1016/j.humpath.2006.01.015.
[34] R.H. Lohr, B.J. Boland, W.W. Douglas, D.H. Dockrell, T.V. Colby, S.J. Swensen, P. C. Wollan, M.D. Silverstein, Organizing pneumonia. Features and prognosis of cryptogenic, secondary, and focal variants, Arch. Intern. Med. 157 (1997) 1323–1329.
[35] H. Oiwa, A. Maeda, T. Nishisaka, Y. Yamanishi, S. Yamana, A. Takanashi, A case of polymyositis complicated with organizing pneumonia: case report and literature review, Mod. Rheumatol. 14 (2004) 388–393, https://doi.org/10.1007/s10165-004-0328-z.
[36] S.A. Yousem, K. Gibson, N. Kaminski, C.V. Oddis, D.P. Ascherman, The pulmonary histopathologic manifestations of the anti-Jo-1 tRNA synthetase syndrome, Mod. Pathol. 23 (2010) 874–880, https://doi.org/10.1038/modpathol.2010.65.
[37] T. Kobayashi, M. Kitaichi, K. Tachibana, Y. Kishimoto, Y. Inoue, T. Kagawa, T. Maekura, C. Sugimoto, T. Arai, M. Akira, Y. Inoue, A cryptogenic case of fulminant fibrosing organizing pneumonia, Intern. Med. 56 (2017) 1185–1191, https://doi.org/10.2169/internalmedicine.56.7371.
[38] R. Nakashima, Y. Imura, S. Kobayashi, N. Yukawa, H. Yoshifuji, T. Nojima, D. Kawabata, K. Ohmura, T. Usui, T. Fujii, K. Okawa, T. Mimori, The RIG-I-like receptor IFIH1/MDA5 is a dermatomyositis-specific autoantigen identified by the anti-CADM-140 antibody, Rheumatology 49 (2010) 433–440, https://doi.org/10.1093/rheumatology/kep375.
[39] H. Kato, O. Takeuchi, S. Sato, M. Yoneyama, M. Yamamoto, K. Matsui, S. Uematsu, A. Jung, T. Kawai, K.J. Ishii, O. Yamaguchi, K. Otsu, T. Tsujimura, C.-S. Koh, C. Reis e Sousa, Y. Matsuura, T. Fujita, S. Akira, Differential roles of MDA5 and RIG-I helicases in the recognition of RNA viruses, Nature 441 (2006) 101–105, https://doi.org/10.1038/nature04734.
[40] A.A. Benitez, M. Panis, J. Xue, A. Varble, J.V. Shim, A.L. Frick, C.B. López, D. Sachs, B.R. tenOever, In vivo RNAi screening identifies MDA5 as a significant contributor to the cellular defense against influenza a virus, Cell Rep. 11 (2015) 1714–1726, https://doi.org/10.1016/j.celrep.2015.05.032.